Journal of Applied Physics

Φ memristor: Real memristor found

Cite as: J. Appl. Phys. **125**, 054504 (2019); https://doi.org/10.1063/1.5042281
Submitted: 31 May 2018 . Accepted: 18 January 2019 . Published Online: 07 February 2019

Frank Z. Wang, Ling Li, Luping Shi, Huaqiang Wu, and Leon O. Chua

Journal of Applied Physics ARTICLE scitation.org/journal/jap

Φ memristor: Real memristor found

Cite as: J. Appl. Phys. **125**, 054504 (2019); doi: 10.1063/1.5042281
Submitted: 31 May 2018 · Accepted: 18 January 2019 ·
Published Online: 7 February 2019

View Online Export Citation CrossMark

Frank Z. Wang,[1,2,3,a)] Ling Li,[1] Luping Shi,[2] Huaqiang Wu,[3] and Leon O. Chua[4]

AFFILIATIONS

[1]School of Computing, University of Kent, Canterbury CT2 7NF, United Kingdom
[2]Brain-like Computing Center, Tsinghua University, Beijing 100084, China
[3]Institute of Micro-Electronics/Beijing Innovation Center for Future Chips, Tsinghua University, Beijing 100084, China
[4]Department of Electrical Engineering and Computer Science, University of California, Berkeley, California 94720-1770, USA

Note: This paper is part of the Special Topic section "New Physics and Materials for Neuromorphic Computation" published in J. Appl. Phys. 124(15) (2018).

[a)]**Author to whom correspondence should be addressed:** frankwang@ieee.org

ABSTRACT

In this work, we invented the Φ memristor to exhibit the direct flux-charge interaction, in which a wire carrying a controlled amount of current is strung through a magnetic core, and, simultaneously, sensing the possibly induced voltage by the switched flux. This work confirms the existence of the ideal memristor postulated almost 50 years ago. In order to study this and its positive/negative integer-/fraction-order counterparties, the flux-charge relationship (and its approximations), the complete differential conformal transformation, and the complete triangular periodic table of elementary circuit elements are developed. The ideal Φ memristor, fractional memristor, mem-inductor/mem-capacitor, and negative memristor are predicted within the context of this new 3-in-1 memristor physics, and their new synaptic functionalities for a brain-like computer are studied experimentally.

I. NEW MEMRISTOR PHYSICS

In this article, new memristor physics refers to the 3-in-1 physics for an ideal Φ memristor based on the direct interaction between the physical magnetic flux and the physical electric charge. The three components of this physics are the flux-charge relationship (and its approximations), the complete differential conformal transformation, and the complete triangular periodic table of elementary circuit elements. It is new as we are probably the first to design an ideal memristor[1] using an actual magnet from a first principle or *ab initio*. Our developed complete differential conformal transformation is new compared with the traditional (integer-order) differential conformal transformation.[2,3] Our proposed complete triangular periodic table is new compared with Chua's rectangular periodic table of circuit elements[4] and Wang's triangular periodic table of circuit elements.[5]

A. Introduction

Ideal memristor was postulated by Chua almost 50 years ago to relate the magnetic flux and the electric charge.[1] A memristor obeys the state-dependent Ohm's law: $v(t) = M(x)i(t)$, except that the memristance $M(x)$ is not a constant but depends on a dynamical state variable x (note $\frac{dx}{dt} = i$). When $x = q$, it becomes an ideal memristor whose memristance is a function of the charge q.[2] In the HP memristor case, $M(x) = xR_{on} + (1 - x)R_{off}$, where x physically represents the ratio between the length of doped region and the total length of the memristor and R_{on} and R_{off} represent the minimum and maximum resistance of the memristor, respectively.[6]

So far, none of the operating memristors is based on the direct interaction between the physical flux and charge. Skeptics expressed their concerns regarding the lack of a flux-charge interaction. In an attempt to theoretically relate the magnetic flux to devices based on their observation that Chua's equations lack material device properties and Strukov's phenomenological model lacks a magnetic flux term, a "virtual" magnetic flux can be calculated as the flux arising from the ions by solving the equations of the missing magnetic flux.[7] However, critics still argued "The Missing Memristor has Not been Found" (the title of their 2015 paper) in the sense that a real memristor device should be grounded in fundamental

symmetries of basic physics, here electro-magnetism, and "ideal/real/perfect/...memristor" needs magnetism.[8,9]

Before the invention of such a real memristor with the direct interaction between the physical flux "ϕ" and the physical charge "q," it is popular to define "ϕ" and "q" in a purely mathematical way without giving "ϕ" and "q" any physical interpretations.[2] For example, "ϕ" was defined as the time integral of the voltage or the flux linkage. It is worth mentioning that, for the case of memristor, the electric field is not as negligible as for the case of inductance, so even treating the flux linkage as the equivalence of the magnetic flux mathematically is not true.[10]

On the other hand, we do not have any choice/way/method to know what "ϕ" is physically and how "ϕ" and "q" interact physically with each other. For example, Chua had to imagine a physically non-existent memristor with a flux-charge relationship $\varphi = \frac{1}{3}q^3 + q$ in his "Resistance switching memories are memristors" tutorial.[2] Although $\varphi = \frac{1}{3}q^3 + q$ is probably the simplest polynomial function satisfying Chua's three criteria for the ideal memristor [(1) Nonlinear; (2) Continuously differentiable; and (3) Monotonically increasing],[1] it is purely fictitious (For convenience, it is also odd-symmetric and has a non-zero slope while crossing the origin.) without any material and physical basis. As can be seen later in Sec. I C, this "fictitious" flux-charge relationship will lead to a number of "un-natural" results, which demonstrates the importance of introducing a "real-world" memristor.

We strongly believe that, in analogy to the real resistor that interacts directly the physical voltage and current, the real capacitor that interacts directly the physical voltage and charge, and the real inductor that interacts directly the physical current and flux, the world's first real memristor that interacts directly the physical flux and charge is still highly in demands in terms of understanding the real memristor physics and using the memristor as Chua's fourth element to seamlessly, symmetrically fill the gap of the basic circuit element table that has already included the (physical) resistor, capacitor, and inductor.[4]

In our opinion, a "real" physical model is always associated with an "ideal" condition rather than a "non-ideal" one. Historically, there was a shift from Aristotle's theory of gravity (a bowling ball falls faster than a feather in air, which is a "non-ideal" condition) to Galileo's theory of gravity (objects fall with the same acceleration in vacuum, which is an "ideal" condition). The shift from a non-flux-charge paradigm to a flux-charge one in the memristor physics may be somewhat similar to the above.

This article is organized as follows: in Sec. I, we will produce a 3-in-1 physical model: the flux-charge relationship based on the LLG (Landau–Lifshitz–Gilbert) equation[11,12] for an ideal Φ memristor, the complete differential conformal transformation, and the complete triangular periodic table of elementary circuit elements; in Sec. II, the Φ memristor will be experimented; in Sec. III, fractional memristor with the fractional flux-charge interaction[13] will be introduced based on the fractional calculous[14,15] and the STT (Spin-Torque Transfer) memristor[16,17] will be studied as an example; in Sec. IV, mem-inductor and mem-capacitor will be introduced within the context of the Adaptive Neuromorphic Architecture (ANA);[18] and in Sec. V, negative memristor will be predicted within the context of a negative triangular table and its peculiar features associated with "Local Activity" (that was originally defined in the nonlinear electronic circuits theory by explaining the emergence of complex patterns at the edge of chaos and can be generalized in physics, chemistry, biology, and brain research)[19] will be investigated. Out of the above four types of circuit elements with memory (namely, ideal Φ memristor, fractional memristor, mem-inductor/mem-capacitor, and negative memristor), the middle two have already been reported elsewhere by us[13,18] but are still briefly summarized and listed in this article for the history and information integrity. Section I (new memristor physics), Sec. II (Φ memristor), and Sec. V (negative memristor) represent the original research, which have never been published elsewhere.

B. Φ Memristor

We design an ideal Φ memristor to physically exhibit the direct flux-charge interaction, in which a conductor carrying a controlled amount of current is in close proximity to a magnetic lump and, simultaneously, sensing the possibly induced voltage by the switched flux. As shown in Fig. 1, the Oersted field generated by the current i rotates the magnetization $\mathbf{M}$ inside the lump and consequently the switched flux φ induces a voltage v across the conductor, resulting in a changed (equivalent) memristance. Note that the missing magnetism or magnetic flux in other memristors has its role to play here.

The above lump is normally assumed to be magnetically uniaxial anisotropic, i.e., it has only one easy axis. Therefore, the magnetization M of the lump will tend to align with the easy axis, which is an energetically favorable direction of spontaneous magnetization.[20] The corresponding memristor is a two-state charge-controlled ideal memristor, among those resistance-switching memories that are identified as ideal memristors by Chua.[2] Chua also proposed recently a new theorem proving that all non-volatile memristors should exhibit a continuous range of resistances, although one may observe only two distinct resistances in practice, because the device may exhibit a very steep (but continuous) "state-dependent Ohm's law."[21] For those memory/logic applications requiring only two states, the memristor needs to exhibit only two equilibrium states that are sufficiently distinguishable and consumes little energy while switching swiftly between these two states. At both equilibrium states, the memristor does not dissipate any power since $v(t) = d\phi(t)/dt = 0$ and $i(t) = dq(t)/dt = 0$ except during the brief switching time intervals.[2]

In addition to uniaxial anisotropy, a magnetic lump with cubic anisotropy has three or four easy axes.[20] Furthermore, a magnetically isotropic material has no preferential direction for its magnetization unless there is an external magnetic field.[20] Accordingly, it is possible to design an ideal

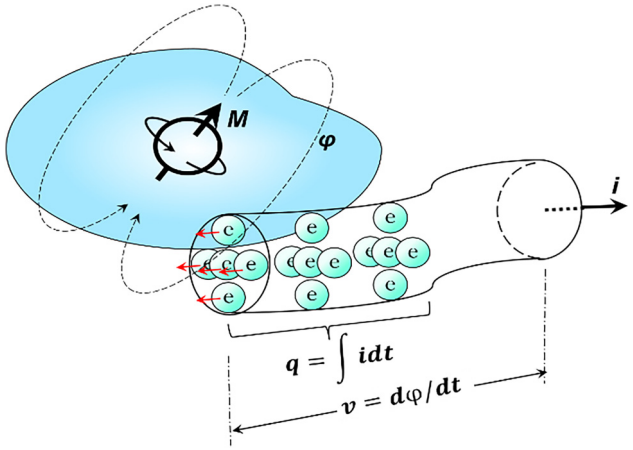

FIG. 1. The Φ memristor based on the direct interaction between the physical flux and charge. The interaction between a magnetic lump and a current-carrying conductor in close proximity to each other is proved to be intrinsically memristive (see the experiments in Sec. II for details). The Oersted field generated by the current i rotates or switches the magnetization $\boldsymbol{M}$ inside the lump and consequently the switched flux φ induces a voltage v across the conductor, resulting in a changed (equivalent) memristance. Following this invention, we named it Φ memristor or Φ/q memristor in a symbolic way: the ring in "Φ" represents a magnetic lump (e.g., a magnetic core) and the vertical bar in "Φ" represents a wire going through that lump (core); on the other hand, Φ often denotes the magnetic flux that is thought to be missing in the ideal memristor. Note that this structure can be reduced to "one body": instead of using the two objects (a magnetic lump and a current-carrying conductor), we can use only one object that is a ferromagnetic conductor with an input current directly flowing through its two terminals, which does not violate the memristive principle (see Fig. 21).

memristor with multi/infinite-stable states for both digital and analog applications.

The necessity of including magnetic materials in a physical memristor is twofold: Firstly, none of the operating memristors so far is based on the interaction between the physical magnetic flux and the physical electric charge although the memristor, by its original definition of ideal memristor[1] in 1971, should relate these two physical attributes. In other memristors reported after the HP seminal publication,[6] either the physical magnetic flux or the physical electric charge (or both) is missing. Secondly, the introduction of magnetic material with rich hysteresis provides a good source of nonlinearity for memristor that should be a nonlinear circuit element.[1]

The above design is different from other (binary) memristors [namely, ReRAM (Resistive Random-Access Memory),[22] STT-RAM,[16,17] and MTJs (Magnetic tunnel junctions)[23]]: (1) The Φ memristor is an ideal memristor, whereas others are not (due to the existence of the hard magnetic layer, for example, see Sec. III for details); (2) The structure of the Φ memristor is much simpler as it only has a (one-body) magnetic lump, whereas others have at least three layers (e.g., hard magnetic/insulator/soft magnetic); (3) The memristance of the Φ memristor results from the interaction between the lump and the current-carrying conductor, whereas others' memristance from the interaction between those multi-layers; (4) The Φ memristor is so far at a macroscopic scale and potentially at a nano-scale (see Sec. VI), whereas others at a nano-scale only.

One reason why it took 37 years for us to see the HP memristor after Chua formulated and named the memristor in 1971 is because the HP memristor phenomena [the memory-holding ionic current (oxygen vacancies)] is only observable in the nano-scale.[6] Although such a nano-scale attribute is essential for the IC industries, the memristor should also be a commercially available off-the-shelf basic circuit element for designing macro-scale (mundane-size) intelligent circuits and systems. Therefore, our Φ memristor will hopefully fulfil this need as its physical size can scale up from the nm to the mm/cm scale (see Sec. II for details).

Prodromakis unearthed that memristors made even in the Victorian era are macro-scale.[24] Other macro-scale memristors include: organic memristor by Erokhin *et al.*,[25] a real memristor circuit for the experimental demonstration of chaos by Gambuzza *et al.*,[26] and a physically flexible T_iO_2 memristor device by Gergel-Hackett *et al.*[27] As pointed out by an anonymous reviewer, we are not the first person to make a macroscopic scale memristor, but we may be the first to do so using an actual magnet.

C. Physics of the Φ memristor

Next, we will produce a theory to describe physically the flux-charge interaction. Suppose that the lump is a single-domain cylinder with uniaxial anisotropy in the approximate sense: the magnetization is uniform and rotates in unison.[28] In an ideal case, it is assumed that there is a negligible amount of eddy current damping and any parasitic capacitor effects.

It is found that the rotational process dominates in the fast reversal of square loop ferrites (a switching coefficient, S_W, of about 0.2 Oe μs is the minimum value obtainable with the materials that have normal gyromagnetic ratios).[29] The corresponding rotational model for our Φ memristor is shown in Fig. 2, where the easy axis is along the Z axis, M_Z is the component of the saturation magnetization M_S in the Z axis, and the magnetic field H is applied in the Z direction.

Let us write the Landau–Lifshitz–Gilbert equation as follows:

$$(1+g^2)\frac{d\vec{\mathbf{M}}_{\mathbf{S}}(t)}{dt} = -|\gamma|[\vec{\mathbf{M}}_{\mathbf{S}}(t)\times\vec{H}] - \frac{g|\gamma|}{M_S}[\vec{\mathbf{M}}_{\mathbf{S}}(t)\times(\vec{\mathbf{M}}_{\mathbf{S}}(t)\times\vec{H})],$$

where g is the Gilbert damping parameter and γ is the gyromagnetic ratio.

The 1st term of the right-hand side can be re-written as $-|\gamma|\,\vec{\mathbf{M}}_{\mathbf{S}}(t)\times\vec{H} = -|\gamma|(M_S\sin\theta\sin\psi H\vec{i} - M_S\sin\theta\cos\psi H\vec{j})$. Note this term does not have any $\vec{k}$ component (along the Z axis) and does not contribute to M_Z.

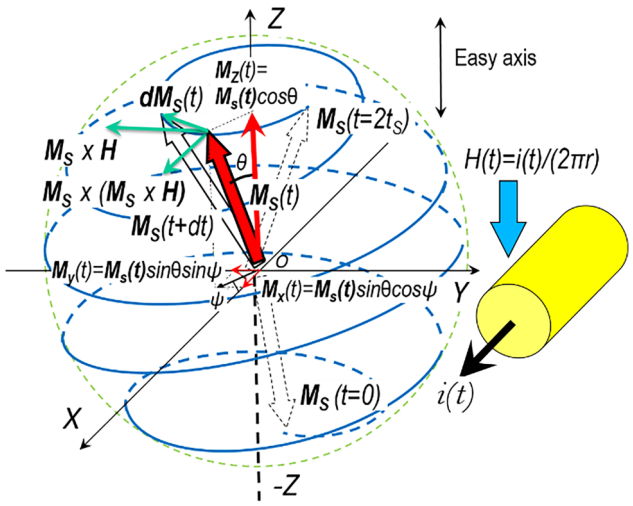

FIG. 2. The rotational model of flux reversal used in our Φ memristor. If the magnetic field $\boldsymbol{H}$ is applied in the Z direction, the saturation magnetization vector $\boldsymbol{M_S}(t)$ follows a precession trajectory (blue) from its initial position ($\theta_0 \approx \pi$, $m_0 \approx -1$) and the angle θ decreases with time continuously until ($\theta \approx 0$, $m \approx 1$), i.e., the magnetization $\boldsymbol{M_S}(t)$ reverses itself and is eventually aligned with the magnetic field $\boldsymbol{H}$.

The 2nd term of the right-hand side can be re-written as

$$
\begin{aligned}
&-\frac{g|\gamma|}{M_S}[\vec{\mathbf{M_S}}(t)\times(\vec{\mathbf{M_S}}(t)\times\vec{H})]\\
&=-\frac{g|\gamma|}{M_S}(M_S\sin\theta\cos\psi\,\vec{i}+M_S\sin\theta\sin\psi\,\vec{j}+M_S\cos\theta\vec{k})\\
&\qquad\times[M_S\sin\theta\sin\psi H\vec{i}-M_S\sin\theta\cos\psi H\vec{j}]\\
&=-\frac{g|\gamma|}{M_S}[-M_S\sin\theta\cos\psi M_S\sin\theta\cos\psi H\\
&\qquad-M_S\sin\theta\sin\psi M_S\sin\theta\sin\psi H]\vec{k}\\
&=g|\gamma|M_S H[\sin^2\theta\cos^2\psi+\sin^2\theta\sin^2\psi]\vec{k}=g|\gamma|M_S H\sin^2\theta\vec{k}\\
&=g|\gamma|M_S H(1-\cos^2\theta)\vec{k}=g|\gamma|M_S H\left[1-\left(\frac{M_Z}{M_S}\right)^2\right]\vec{k}.
\end{aligned}
$$

From the above, we should obtain the following equation:

$$(1+g^2)\frac{dM_Z(t)}{dt}=g|\gamma|M_S H\left[1-\left(\frac{M_Z}{M_S}\right)^2\right]. \tag{1}$$

Assuming $m(t)=\frac{M_Z(t)}{M_S}$, we obtain

$$\frac{dm(t)}{dt}=\frac{g|\gamma|H}{(1+g^2)}[1-m^2(t)]=\frac{1}{S_W}i(t)[1-m^2(t)], \tag{2}$$

where S_W is the aforementioned switching coefficient. The threshold for the magnetization switching is automatically taken into account because the switching coefficient is defined based on the threshold field H_0, which is of one to two times the coercive force H_C.[29–31]

The hyperbolic function tanh has $\frac{d}{dx}\tanh x=1-\tanh^2 x$ and the derivative of a function of function has $\frac{du}{dx}=\frac{du}{dy}\frac{dy}{dx}$; therefore, it is reasonable to assume

$$m(t)=\tanh\left[\frac{q(t)}{S_W}+C\right], \tag{3}$$

where $\frac{d}{dt}q(t)=i(t)$ and C is a constant of integration such that $C=\tanh^{-1}m_0$ if $q(t=0)=0$ (assuming the charge does not accumulate at any point) and m_0 is the initial value of m.

dM_z/dt is observed by the voltage $v(t)$ induced in the conductor

$$\mu_0 S\frac{dM_z}{dt}=S\frac{dB_z}{dt}=\frac{d\varphi_z}{dt}=-v(t), \tag{4}$$

where μ_0 is the permeability of free space and S is the cross-sectional area.

From Eq. (4), we obtain

$$\varphi=\mu_0 SM+C'=\mu_0 SM_S m+C', \tag{5}$$

where C' is another constant of integration.

Combining Eqs. (3) and (5) and assuming $\varphi(t=0)=0$, we have $C'=-\mu_0 SM_S m_0$, so

$$\varphi=\mu_0 SM_s\left[\tanh\left(\frac{q}{S_W}+\tanh^{-1}m_0\right)-m_0\right]\triangleq\hat{\varphi}(q). \tag{6}$$

Equation (6) complies with the new three criteria[32] for the ideal memristor: (1) Nonlinear; (2) Continuously differentiable; and (3) Strictly monotonically increasing. Figure 3 shows a typical φ-q curve with $m_0=-0.964$ ($\theta_0\approx\pi$) due to the intrinsic fluctuation otherwise $\mathbf{M}$ will be stuck at stable equilibrium magnetization states $\theta=0$ or π ($m_0=\pm1$).

The remarkable resemblance between Fig. 3 and those experimentally observed φ-q curves in the magnetic cores[29–31] inspires us to henceforth use Eq. (6) as a "real-world" memristor's constitutive curve in this article. As shown in Fig. 3, it is quite different from that of Chua's "fictitious" memristor with a flux-charge relationship $\varphi=\frac{1}{3}q^3+q$.[2] We have $\lim_{q\to\pm\infty}\tanh(q)=\pm1$ for a hyperbolic function whose output range is normalized from –1 to 1 no matter how big the input is whereas $\lim_{q\to\pm\infty}\left(\frac{1}{3}q^3+q\right)=\pm\infty$ for a polynomial function (that diverges to infinity). In other words, our "real-world" memristor's operation range is finite [where $M(q)=\frac{d\varphi}{dq}\neq0$], whereas the "fictitious" memristor's range is infinite. It seems that the former is more natural than the latter. As a matter of fact, in artificial neural networks, the tanh activation function is biologically reflected in the neuron (it stays at zero until input current is received, increases the

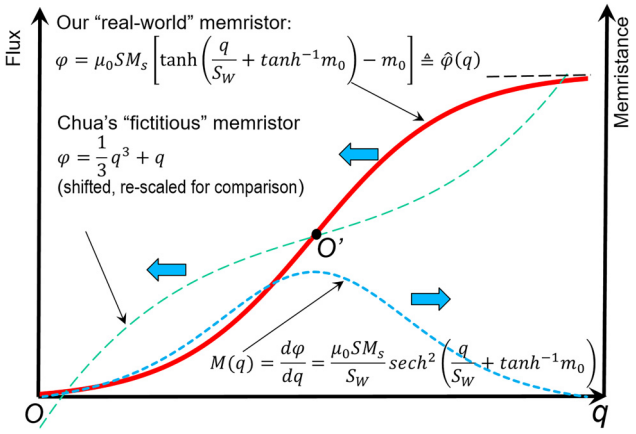

FIG. 3. The φ-q curve for the "real-world" (charge-controlled) memristor in comparison with that for a "fictitious" one.[2] The (switched) flux φ that occurs in a magnetic lump depends only on the effective charge q that has flowed through the conductor and the initial state of magnetization.

slope (firing frequency) quickly at first, but gradually approaches an asymptote at 100% firing rate). Physically, we can give a clear explanation for the saturation of the "real-world" memristor. As shown in Fig. 2, such a saturation is because the magnetization vector is as aligned as the external magnetic field allows it to be, so there is a negligible change in the magnetization alignment on increasing the field above this.

The above continuous differentiable $\hat{\varphi}(q)$ curve may be approximated by piece-wise-linear segments for convenience. Different types of functions will result in different slope (memristance) distributions in their piece-wise-linear approximations: it is low-high-low for tanh(q), whereas high-low-high for $\frac{1}{3}q^3 + q$ (a piece-wise-linear charge-controlled "fictitious" memristor in Fig. 5 of the tutorial[2] has such "unnatural" high-low-high memristance distribution). The physical explanation for the "real-world" memristor with a large memristance on the middle segment is the magnetization $\mathbf{M_s}$ will swiftly cross "the equator of the earth" ($\theta = \pi/2$, an unstable equilibrium, see Fig. 2), inducing a large flux change, if a new equilibrium is not sustained.

No deep physical understanding would be possible even for the tutorial purpose unless a memristor is modeled properly, accurately. The above deduced $\hat{\varphi}(q)$ function [Eq. (6)] is so important that it will guide the design of an ideal Φ memristor (Sec. II) and its piece-wise-linear approximation will also be used in the design of fractional memristor, mem-conductor/mem-capacitor, and negative memristor (Secs. III–V).

If a step-function excitement current is applied and its rise time is short enough in approaching constant I, by Faraday's law, the induced voltage is

$$v(t) = \frac{d\varphi}{dt} = \frac{\mu_0 SM_S I}{S_W} \mathrm{sech}^2\left(\frac{I}{S_W}t + \tanh^{-1}m_0\right). \quad (7)$$

Equation (7) is depicted in Fig. 4.

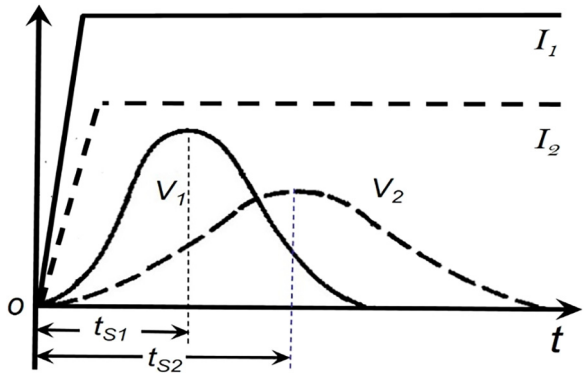

FIG. 4. Induced voltage vs a step-function input current. The higher the amplitude of the current I, the shorter the switching time t_s.

From Eq. (6), the memristance M(q) of our Φ memristor is

$$\mathrm{M}(q) = \frac{d\varphi}{dq} = \frac{\mu_0 \mathrm{SM_s}}{\mathrm{S_W}} \mathrm{sech}^2\left(\frac{q}{\mathrm{S_W}} + \tanh^{-1}m_0\right) \geq 0. \quad (8)$$

From Eq. (8), we should have the following passivity criterion:

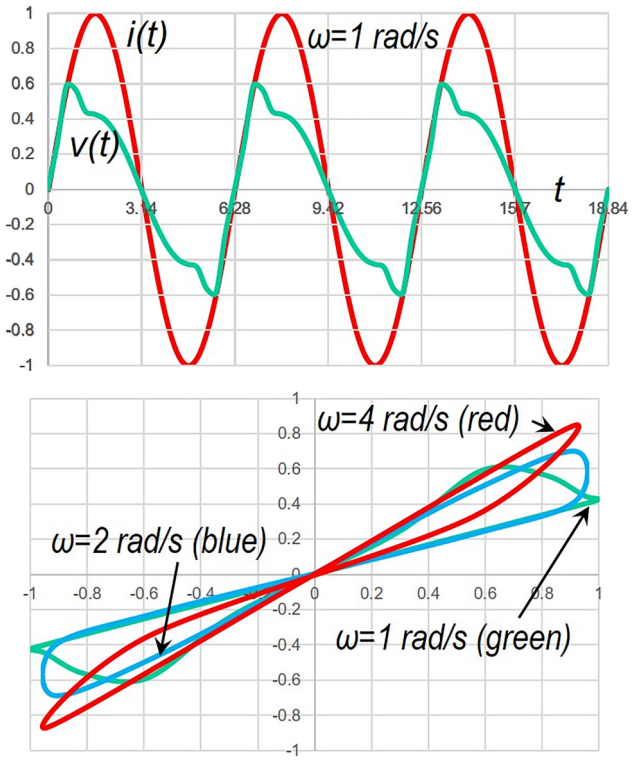

FIG. 5. Pinched hysteresis loops for $A = 1$, $S_W = 0.3$ Oe μs and $\omega = 1$, 2, and 4 rad/s. Hysteresis occurs because the maxima and minima of $v(t)$ do not occur at the same time as that of $i(t)$.

Theorem I: Passivity Criterion

The Φ memristor is passive.

Proof: Equation (8) shows clearly the slope of $\hat{\varphi}(q)$ is non-negative (also see Fig. 3), and hence this Φ memristor is locally passive at each point on the ϕ-q curve.

This criterion is important for small-signal circuit analysis since a locally active memristor may give rise to oscillations, and even chaos.[2,19] Local activity and negative memristor will be discussed in Sec. V.

So far, we found a physical model and the state equation for this (charge-controlled) Φ memristor: Eq. (8) (depicted in Fig. 3) is viewed as the state-dependent resistance of the associated Ohm's law, and $dq/dt = i$ is the state equation [$i(t)$ is an arbitrary driving function].

From Eq. (8), it can be seen that the above flux-charge interaction is intrinsically memristive.

From Eq. (8), it can also be seen that the memristance $M(q)$ is continuous and reaches its peak value when $\frac{q}{S_W} + \tanh^{-1} m_0 = \frac{I}{S_W} t + \tanh^{-1} m_0 = 0$

$$M_{max} = \frac{\mu_0 S M_s}{S_W}. \tag{9}$$

This maximum occurs at the switching time t_s, which provides the correct time point to measure the (maximum) memristance (for potential memory/switch applications)

$$t_s = -\frac{S_W}{I} \tanh^{-1} m_0. \tag{10}$$

As shown in Fig. 4, the switching time t_s in Eq. (10) is inversely proportional to the amplitude of the input current I.

Most importantly, Eqs. (6)–(10) illustrate vividly the direct flux-charge interaction in Fig. 1: a flux in the lump needs to be switched by a minimum amount of charge. Note that it is the charge q that controls the switching. A strong current, or a strong magnetic field, cannot switch the lump without a minimum time interval (t_S corresponding to $\theta = \pi/2$). The switching time t_S is such a critical point that, beyond $\pi/2$, θ will precess with decreasing amplitude until **M** has reversed by π.

The theoretically determined and experimentally validated flux-charge curves can adequately represent the switching action and can be easily related to circuit applications. It is possible to predict the response voltage to an arbitrary input current source. For example, let us apply a sinusoidal current source defined by $i(t) = \begin{cases} A \sin(\omega t), & t \geq 0 \\ 0, & t < 0 \end{cases}$ across this memristor. As $q(0) = 0$, we obtain $q(t) = \int_0^t i(\tau) d\tau = A/\omega[1 - \cos(\omega t)]$, $t \geq 0$.Substituting it into Eq. (6), we obtain

$$\varphi(t) = \mu_0 S M_s \left(\tanh\left\{ \frac{A}{\omega S_W} [1 - \cos(\omega t)] + \tanh^{-1} m_0 \right\} - m_0 \right). \tag{11}$$

Differentiating Eq. (11) with respect to t, we obtain

$$v(t) = \frac{d\varphi}{dt} = \mu_0 S M_s A \operatorname{sech}^2 \times \left(\tanh\left\{ \frac{A}{\omega S_W} [1 - \cos(\omega t)] + \tanh^{-1} m_0 \right\} \right) \sin(\omega t). \tag{12}$$

As shown in Fig. 5, we found that hysteresis occurs because the maxima and minima of $v(t)$ do not occur at the same time as that of $i(t)$. The fact that both the sinusoidal current $i(t)$ and the modulated-sinusoidal voltage $v(t)$ become zero at the same time means they are pinched at the origin, which is the fingerprint of all memristors.[3]

D. Our complete differential conformal transformation

As part of our new memristor physics, we re-developed the traditional differential conformal transformation and named it the complete differential conformal transformation. What we mean by "complete" is that our new transformation covers not only the (traditional) integer-order but also the fraction-order. The complete transformation will use the above deduced flux-charge formula [Eq. (6)].

Figure 6 illustrates our complete differential conformal transformation: the above deduced φ–q curve for an ideal memristor in the φ–q plane in (c) is projected onto the v-i (voltage-current) plane in (d) and M-i (memristance-current) plane in (b) via q-t in (e) and i-t in (f). We can draw the voltage-current loci $v = \hat{v}(i)$ corresponding to the above given $\varphi = \hat{\varphi}(q)$ curve: (1) Get the angle of incline β of the tangent line at an operating point in the $\varphi = \hat{\varphi}(q)$ curve and draw a straight line through the origin in the v-i plane whose angle of incline is $\beta' = \beta$; (2) Project the point from the φ–q plane onto the v-i plane (by following Projection Lines ①, ②, and ③); (3) By meeting Projection Line ③ with the line drawn in the first step, get the same time point in the v-i plane [Fig. 6(d)] and the M-i plane [Fig. 6(b)].

If the sinusoidal current source $i(t) = A \sin(\omega t)$ is applied across the memristor, the corresponding memristor charge is given by $q(t) = \frac{d^{-\alpha}}{dt^{-\alpha}} i(t) = \frac{d^{-\alpha}}{dt^{-\alpha}} A \sin(\omega t) = A\omega^{\alpha}\left[1 - \sin\left(\omega t + \frac{\alpha}{2}\pi\right)\right]$, where $\frac{d^{-\alpha}}{dt^{-\alpha}}$ is the fraction-order calculus operator ($0 \leq \alpha \leq 1$). The introduction of the fraction-order calculus here is to describe some non-ideal memristors whose flux-charge-coupling is fractional (see Sec. III for details). Note that a sinusoidal input is used here without losing the generality because any periodic function can be decomposed into Fourier series of sines and cosines. Furthermore, our theory [centered around Eq. (6)] even does not stop one from applying a non-periodic input as long as they think using a non-periodic signal is necessary and beneficial for their tests. Then, based on the derivative of a function of function, we have a generic expression for the complete transformation (including both the fraction-order and negative cases) as follows:

$$v(t) = \frac{d^{\alpha}}{dt^{\alpha}} \varphi(t) = \frac{d^{\alpha} \hat{\varphi}(q)}{dq^{\alpha}} \frac{d^{\alpha} q(t)}{dt^{\alpha}} = M_{\alpha}[q(t)] i(t), \tag{13}$$

where $M_{\alpha}(q)$ is the memristance in the fraction-order.

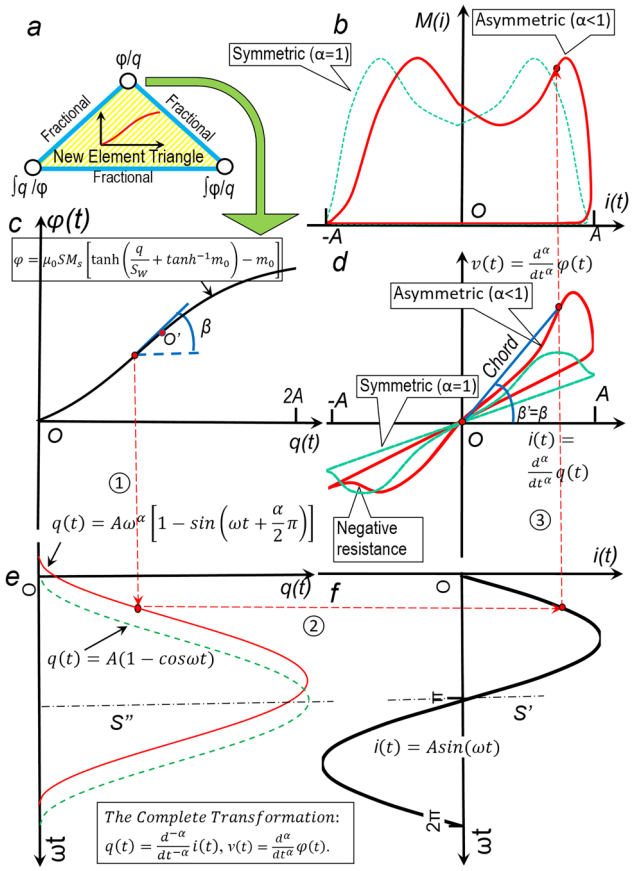

FIG. 6. The complete differential conformal transformation. It projects the above deduced φ–q curve for an ideal memristor in the φ–q plane in (c) onto the v-i plane in (d) and M-i plane in (b) via (e) and (f). This transformation is complete since it covers all cases in this article: $\alpha = 1$ corresponding to a (positive) ideal memristor (Sec. II); $-1 < \alpha < 1$ corresponding to a (positive/negative) fractional memristor [Sec. III, the shift of $q(t)$ along the t axis in (e) results in both the asymmetric v-i loci in (d) and M-i loop in (b)]; mem-inductor/mem-capacitor can be characterized in their own constitutive planes in a similar way (Sec. IV); $\alpha = -1$ corresponding to a negative (ideal) memristor (Sec. V, the φ-q curve enters the 2nd and 4th quadrants of the φ-q space). The two physical attributes, φ and q, will bridge this transformation and a complete triangular element table in (a) (to be elaborated in Fig. 7).

As can be seen in Fig. 6, $q(t)$ shifts by $(\alpha/2)\pi$ along the t axis with respect to $i(t) = A\sin(\omega t)$, which will lead to the asymmetric hysteresis loop in the v-i plane [Fig. 6(d)] and the asymmetric memristance hysteresis loop in the M-i plane [Fig. 6(b)]. Such an asymmetry (unequal switching currents $|I_c^+| \neq |I_c^-|$) is worth studying in depth. It manifests the difference between the switching current from the low-resistance state to the high-resistance state and the one from high to low, as shown in Fig. 6(b). This asymmetry may increase the complexity of the peripheral circuit design and compromise the reliability of operation in neuromorphic computation engineering. Theoretically, we should have the following criterion:

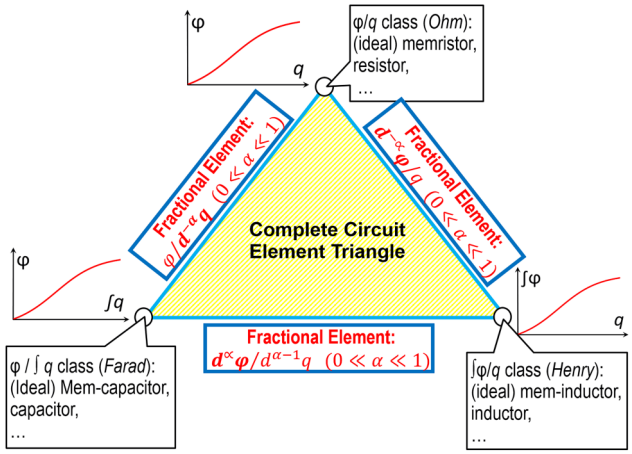

FIG. 7. The complete triangular periodic table of elementary circuit elements. φ and q used in the complete differential conformal transformation (Fig. 6) are thought to be a pair of complementary basic attributes that generate elementary circuit elements. Each apex represents an exclusive class of elements (namely, ideal memristor, ideal mem-inductor, and ideal mem-capacitor). The intermediate case between the apexes represents fractional memristors. This triangle can infinitely be expanded inwards and outwards to have those apexes' higher order or lower order counterparts. Note that negative elements are not included by this (positive) triangle because it is purely a collection of passive elementary circuit elements. As can be seen in Fig. 15, this (positive) triangle can be projected onto a screen in the negative space to obtain a negative triangle of those negative elements.

Theorem II: Symmetry Criterion

The (charge-controlled) Φ memristor has an odd-symmetric voltage-current hysteresis loop and a symmetric memristance hysteresis loop if it is driven by an odd-symmetric periodic excitement current.

Proof: The memristance as a function of time is a function $M(q)$ of function $q(t)$. As can be seen in Fig. 6, when $\alpha = 1$, $q(t)$ is symmetric about S'' [as it is the integral of an odd-symmetric function $i(t)$ about S'] and the ϕ-q curve [determined by Eq. (6)] is odd-symmetric about O'. Therefore, the memristance as the slope of the ϕ-q curve must be a symmetric function (Fig. 3) and the memristance hysteresis loop $M(i)$ is therefore symmetric as it is driven by the odd-symmetric excitement current $i(t)$. From Eq. (13), the response voltage $v(t)$ must be odd-symmetric and hence the v-i loci is also odd-symmetric about O. Obviously, this symmetry will be broken when $\alpha < 1$ since the shifting charge $q(t)$ is not symmetric about S'' any longer.

In Fig. 6(c), the differential memristance is defined as the derivative of the flux with respect to the charge or the ratio of a small change in flux to the corresponding change in charge in the ϕ-q plane; in Fig. 6(d), the chord memristance is defined as the slope of a straight line connecting the corresponding point to the origin in the v-i plane.[2]

Actually, the projection from the φ-q plane to the v-i plane in Fig. 6 is based on the following theorem:

Theorem III: Conformality Criterion

The complete differential transformation that covers both integer-order and fraction-order is conformal.

Proof:

$$\beta = \text{arctg}\left(\frac{d^{\alpha}\hat{\varphi}(q)}{dq^{\alpha}}\right) = \text{arctg}\left(\frac{\frac{d^{\alpha}}{dt^{\alpha}}\hat{\varphi}(q)}{\frac{d^{\alpha}}{dt^{\alpha}}q(t)}\right) = \text{arctg}\left(\frac{v(t)}{i(t)}\right) = \beta'.$$

That is to say, the differential transformation in the fraction-order still preserves angles in the same way as the (traditional) integer-order transformation does. This is why we named "the complete conformal differential transformation." Obviously, the (differential) memristance of a point on the ϕ-q curve equals the chord memristance of the corresponding point on the v-i curve in the complete transformation.

Typically, Fig. 6(d) is a pinched hysteresis loop, i.e., it passes through the origin. It also displays a double-valued Lissajous figure [$v(t)$-$i(t)$] for all times t. Obviously, the fingerprint of a memristor[3] can be seen.

These pinched hysteresis loops contain a small region with a negative slope. The negative slope just indicates a phase-lag between the peak of the response voltage $v(t)$ and the peak of its excitation current $i(t)$ and is irrelevant to the local activity.[2,19] Local activity and negative memristance will be discussed in detail in Sec. V.

Note that our transformation does characterize a memristor's behavior by the flux-charge relationship [as shown in Fig. 6(c) and Eq. (6)] and it is such a universal tool that all waveforms are covered. Although a sinusoidal input is used in Fig. 6(f), our transformation is not constrained to any specific signal at all. In the same manuscript, we will use at least four different waveforms: a sinusoidal input, a triangular input, a square-wave input, and a sequence of spikes.

E. Our complete triangular periodic table of elementary circuit elements

As part of our new memristor physics, we will build a complete triangular circuit element table (Fig. 7) based on the above complete transformation. The two physical attributes, φ and q, will bridge the transformation and the table: on the one hand, they are used in the complete differential conformal transformation as two dimensions of the constitutive plane; on the other hand, they generate elementary circuit elements as a pair of complementary basic attributes in the circuit element table.

A two-terminal elementary electronic circuit element should link two physical attributes (φ or q and their derivatives), at least one of which should be physically intrinsic and basic. It is our opinion that, within a certain context, φ and q should be more basic than v and i.[5] Physically, the magnetic flux and the electric charge are fundamental features associated with the material and physical mechanism in terms of describing an object. Contrarily, the voltage and current could be derived from the flux and charge. Furthermore, although conveniently used in engineering applications, the voltage and current only exhibit external measurements of an object (e.g., the voltage v is always a "difference" and the current i is always the movement of charge q).[5]

Sharing the same SI unit, the three apexes of the triangle represent three exclusive classes of elements [namely, ideal memristor (the φ/q class), ideal mem-inductor (the $\int\varphi/q$ class), and ideal mem-capacitor (the $\int q/\varphi$ class)]. As an exception, the element linking $\int\varphi$ and $\int q$ should not be elementary because both $\int\varphi$ and $\int q$ are derived (from the basic attributes ϕ and q mathematically). The exclusion of $\int\varphi/\int q$ is decisive otherwise the Chua's quadrangle (based on v, i, ϕ, and q)[4] will not collapse to a triangle (based on ϕ and q only).[5]

This triangular table is new as it is extended to include more circuit elements: the intermediate case between the apexes (the integer-order elements) represents fractional memristors, in which the interaction between the flux and charge is fractional (see Sec. III for details); the positive triangle in Fig. 7 can be projected onto a screen in the negative space to obtain a negative triangle of those genitive elements, as can be seen in Fig. 15.

In our opinion, the importance of predicting new circuit elements via an element table is similar to that of Mendeleev's periodic table of chemical elements in chemistry and the table of 61 elementary particles in physics. Note that the above element tables (no matter whether it is rectangular or triangular) can infinitely be expanded inwards and outwards to have those apexes' higher order or lower order counterparts. High-order memristors may be unusual but still exist. For example, the two time-varying resistors approximated by Hodgkin and Huxley 70 years ago in their famous Nobel-prize-winning Hodgkin–Huxley axon circuit model were eventually found to be a first-order memristor for the potassium ion channel and a second-order memristor for the sodium ion channel.[33]

Next, we will use the above physics to study a number of memristors and study their potential applications in neuromorphic computation.

II. Φ MEMRISTOR

As the first attempt of the above new memristor physics, the Φ memristor will be investigated experimentally. A magnetic core with a wire passing through it (inset of Fig. 8) is used as a Φ memristor. In principle, the magnetic lump in the Φ memristor can take any shape, e.g., a ball, slab, ring, or barrel. The shape matters in terms of the efficiency of the magnetism-electricity coupling. As can be imagined, any "closed" shape (e.g., a ring) encircling the conductor can couple magnetism and electricity more efficiently than those "open" shapes (e.g., a ball). However, there are two sides to everything. Such a "closed" structure may bring in a side-effect—the parasitic "inductor" effect.

In the experimental apparatus, the wire carries a controlled amount of current and simultaneously senses for the possible emergence of an induced large transient voltage response. Different from a standard magnetic core memory cell with several wires (typically two X/Y lines for coincident-currents plus one sense/inhibit line), this device is a two-terminal circuit element.

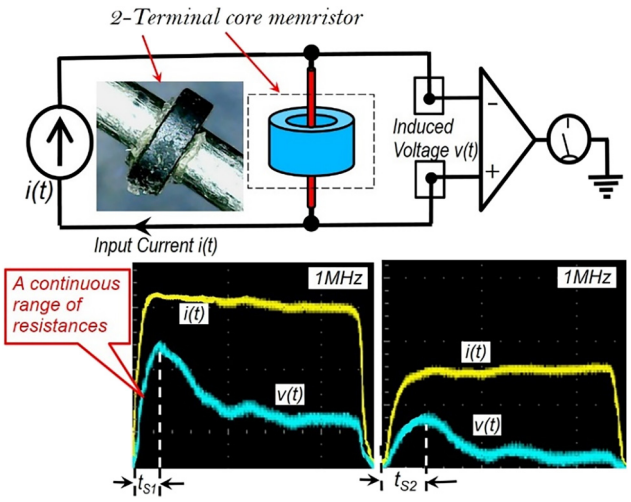

FIG. 8. The experimental apparatus and current pulse responses to verify our Φ memristor model. The induced voltage $v(t)$ against the step function input current $i(t)$ exhibits a steep but continuous "state-dependent Ohm's law." Furthermore, the switching time t_s is inversely proportional to the amplitude of the input current I, which is in an agreement with the theory in Eq. (10) and Fig. 4. Horizontal: 50 ns/div; vertical: 20 mA/div (yellow), and 50 mV/div (blue).

The core (Mn-Cu ferrite with an easy magnetization axis along its circumferential direction and a switching coefficient of 0.25-0.35 Oe μs) has an inside diameter of 0.762 mm, an outside diameter of 1.27 mm, and a height of 0.381 mm (extracted from a 1960s' 64 × 64 bits magnetic core memory purchased from eBay). The wire going through the cores is an enamelled copper wire purchased from Maplin with a diameter of 0.56 mm. Simply speaking, this memristor is a reduced magnetic memory core with only one wire.

A current source (Tektronix MHS-5200P High Precision Digital Dual-channel Signal Generator with attached power amplifiers in series with a cement resistor of 47 Ω 30 W) is designed to deliver $i(t)$ which is independent of the voltage across the core memristor whose equivalent resistance is less than 1 Ω. The two channels are connected in series to double the output voltage of a single channel. The two fixed probes are used to measure the possibly induced voltage $v(t)$ between the two terminals.

Pulse responses against a step function input are observed. As elaborated above, the core can be switched from one of the two states to the other by applying an appropriate current pulse through the wire. Figure 8 shows the induced voltage waveform measured from the same wire carrying an input current. The voltage response exhibits a steep but continuous "state-dependent Ohm's law," just as predicted in Eqs. (7) and (8) (the power of the hyperbolic function sech). A reasonable agreement between the model and the measured waveform can be seen.

In principle, a memristor should exhibit a continuous range of resistances. We notice that both the Φ and spintronic memristors[34] exhibit bi-stable states and a continuous range of resistances. The resistance curve is steep but still continuous, which follows well the "state-dependent Ohm's law" as indicated in Eq. (8). This fact does not surprise us as the magnetic lump in our Φ memristor is equivalent to the "soft" magnetic layer in the spintronic memristor. The difference is the current's driving mechanisms: in our Φ memristor, we use the current's Oersted field to facilitate the flux-charge interaction (satisfying Chua's 1971 definition of ideal memristor[1]), whereas in the spintronic memristor they use the electrons' spin (after a "hard" magnetic layer that filters the spin orientations) to interact with the magnetization (spin) in the "soft" layer.[16,17]

Note that a parasitic "inductor" effect exists in the core structure, which was observed as sharp transient spikes caused by the sudden change of the input current $\left(V_L(t) = L\frac{di(t)}{dt} \neq 0\right)$. Fortunately, this effect is narrowly constrained at the rise/fall edges of the step function. We removed these high-frequency noises by simply using the "compensation adjustment" function (a low-pass filter, LPF) of an oscilloscope (GW Instek GDS-1072B). In the most time of the cycle (especially in the memristive region of our interest), no "inductor" exists as $V_L(t) = L\frac{di(t)}{dt} = 0$.

Definitely, the Φ memristor is neither "an inductor with memory" nor a mem-inductor although there may exist the parasitic "inductor" effect. Actually, in Sec. IV, the uniqueness of those circuit elements with memory is demonstrated in ANA whose (adaptive) time constant $\{\sqrt{L[q(t)]C}\}$ is determined by a mem-inductor (whose inductance is a function of charge).[19] What makes our Φ memristor different from mem-inductor and others is that its resistance is a function of charge [Eq. (8) and Fig. 8]. Experimentally, no capacitive or inductive effects was observed (otherwise there should be a phase shift between the current and voltage) by taking two measures: (1) Using the step function excitement current only and (2) using a low-pass filter that passes signals with a frequency lower than a certain cut-off frequency and attenuates noises with frequencies higher than the cut-off frequency.

As we tested, no voltage was generated when we applied a current through a bare wire without any magnetic core (since an ideal wire has no resistance). It is the magnetization in the core that induces a voltage through its reversal, which has been observed.

Figure 9 shows the complete differential conformal transformation for our ideal Φ memristor ($\alpha = 1$). A square-wave excitement current results in a triangular waveform charge as the charge is the integral of the current. Clearly when the charge is sweeping incrementally, the flux exhibits a cumulative effect as it is the integral of the response voltage [take Eq. (7) and Fig. 4 for reference]. The intrinsic constitutive φ-q curve can then be uniquely determined by the application of the above square waveform current excitement.

As the key mechanism of this ideal memristor, the memristive electricity-magnetism interaction is experimentally verified based on the observed frequency dependence and zero-crossing as follows. The frequency-dependent Lissajous figure reflects a nonlinear relation between the memristor's

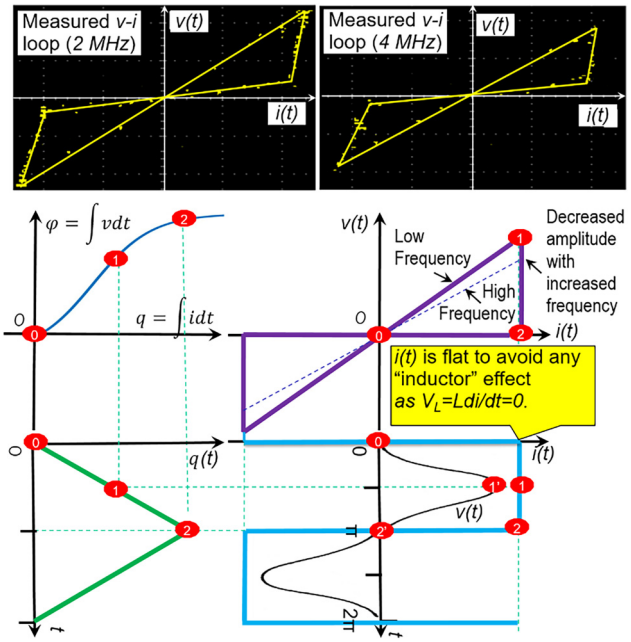

FIG. 9. The complete differential conformal transformation ($\alpha = 1$) for our Φ memristor and the experimentally-verified memristive electricity-magnetism interaction. Two memristor fingerprints can be seen: (1) Frequency dependence; (2) Zero-crossing. Note that a square-wave excitement current is used here since a (continuous) sinusoidal current cannot be used due to the parasitic "inductor" effect in the magnetic core. A careful examination of the photos reveals that the return path ①-② is not ideally vertical to the $i(t)$ axis and this is because the excitement current is not ideally flat. Scales in photos: horizontal: 20 mA/div; vertical: 50 mV/div.

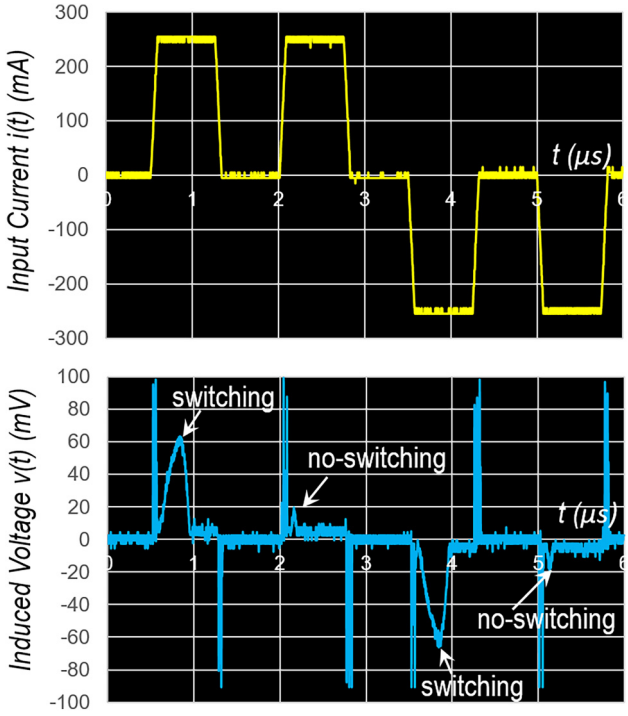

FIG. 10. The measured voltage response against the positive-positive-negative-negative input current pulse pattern. This voltage response exhibits a yes-no-yes-no reversal pattern as anticipated. Horizontal scale is 1 μs/div; Vertical scales are 100 mA/div (upper) and 50 mV/div (lower).

charge and flux. The loop shrinks with increased frequency and such a frequency dependence is a fingerprint of a memristor.[3] Moreover, both the current $i(t)$ and the voltage $v(t)$ are pinched at the origin as expected.[3]

As a result, we experimentally found that the memristive effect is observable and even a simple combination of a magnetic lump and a conductor (Fig. 1) could be an ideal memristor. We claim our new device is an ideal memristor in the sense that it involves only the flux-charge interaction in a classic way (no quantum effect, no spin effect) and is therefore not constrained by its physical size.

Figure 10 shows the measured voltage response against the positive-positive-negative-negative input current pulse pattern. This voltage response should exhibit a yes-no-yes-no reversal pattern because the 1st positive current pulse in the sequence will always switch the core (after many cycles of the periodic excitement), whereas the 2nd one does not since it is opposite to that which would switch the core. In other words, the no-switching state of the core always follows the flux reversal. As can be seen clearly, the voltage waveform of a no-switching core is much smaller (at least 1:3) than that of a switching one, which is vital for reliable memristor operations. Although the response should be zero for a no-switching core in theory, a small signal can still be seen because the core material is not 100% in being magnetically uniaxial anisotropic. The areas of the positive and negative responses are equal, because there is no net change in the flux linkage. One curious reader may want to see the sharp transient spikes caused by the rapid change of the step function input current without using the above mentioned low-pass filter.

Our ideal Φ memristor may help understand better the real physical mechanism of the memristor by interacting directly the flux and charge according to memristor's original definition. From a historical perspective, we note that since our flux-charge-interaction-based Φ memristor is defined basically via Oersted's law, which was discovered by Oersted in 1820,[35] its physical operating principle actually predates that of the resistor, which was formally published by Ohm in 1827,[36] and the inductor, which was formally published by Faraday in 1831.[37]

III. FRACTIONAL MEMRISTOR

Based on the complete differential conformal transformation in the fractional order described in Sec. I, we define the fractional memristor in contrast to the traditional (integer-order) memristor.[2] On the one hand, an (ideal) memristor

(with a φ–q curve shown in Fig. 3, for example) can be approximated by a multi-segment piece-wise-linear curve for convenience. On the other hand, the piece-wise-linear φ–q curve itself represents perfectly the STT memristor with a rectangular memristance R-i curve.

A typical STT memristor (with the asymmetric rectangular resistance hysteresis) is studied as an example. If $\omega = 1$, we have $q(t) = \frac{d^{-\alpha}}{dt^{-\alpha}} i(t) = \frac{d^{-\alpha}}{dt^{-\alpha}} [2Q_0 \cos(\omega t)] = 2Q_0 \cos(\omega t - \frac{\alpha}{2}\pi)$. When the fraction-order $\alpha = 0.8$, $q(t) = 2Q_0 \cos(\omega t - 0.4\pi)$, which is drawn in Fig. 11(e). Obviously, $q(t)$ shifts by 0.4π along the t axis. Such a shift causes an asymmetric shift ($|I_c^+| \neq |I_c^-|$) of the two switching points of the v-i and R-i curves although the breakpoint Q_0 of the φ-q is fixed.

The resemblance between such an asymmetric rectangular R-i curve in Fig. 11 and the measured one in Fig. 12 reveals that a typical STT junction is actually a 0.8 fractional

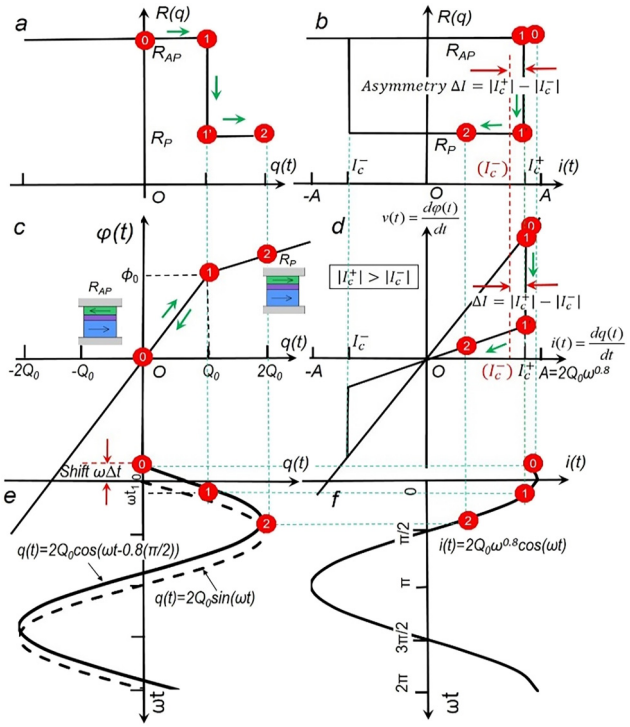

FIG. 11. A special case ($-1 < \alpha < 1$) of the complete differential conformal transformation for fractional memristor. The Symmetry Criterion (Theorem II) and the Conformality Criterion (Theorem III) in Sec. I are used here. When $\alpha = 0.8$, the shift Δt of $q(t)$ along the t axis in (e) causes the asymmetric shifts ($|I_c^+| \neq |I_c^-|$) of the two switching points of the v-i in (d) and R-i or M-i curves in (b) although the breakpoint Q_0 of the φ-q is fixed. Note that the v-i loci in the fractional-order memristor is also a *pinched* hysteresis loop through the origin, which is the fingerprint of a memristor.[2,3] The numbers in red label successive time points. Note the subscripts "P" and "AP" stand for "Parallel" and "Anti-Parallel," respectively. [Reproduced with permission from Wang *et al.*, Appl. Phys. Lett. **111**, 243502 (2017). Copyright 2017 American Institute of Physics.]

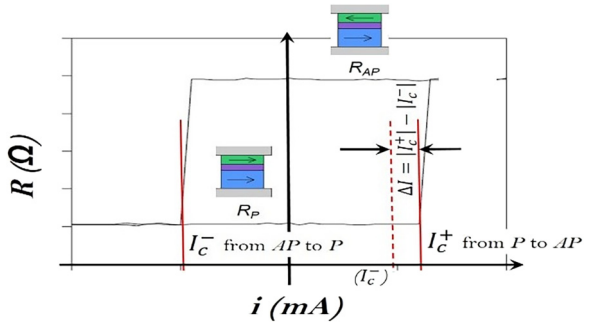

FIG. 12. An asymmetric rectangular R-i curve with two stable, distinct memristances is measured in many STT junctions. Note that a typical R-i curve based on[38–41] shifts by $\Delta I = |I_c^+| - |I_c^-|$ along the i axis. I_c^+ represents the critical current corresponding to the switching from P to AP, whereas I_c^- represents the critical current corresponding to the switching from AP to P. [Reproduced with permission from Wang *et al.*, Appl. Phys. Lett. **111**, 243502 (2017). Copyright 2017 American Institute of Physics.]

memristor. According to our Symmetry Criterion (Theorem II), for an ideal memristor ($\alpha = 1$), there is no asymmetry ($\Delta I = 0$) and it should have a symmetric rectangular M-i curve. With the increase of ω, the asymmetry reaches its maximum at different fractional-orders.[13]

The above conclusion that a STT is a 0.8 fractional memristor means the traditional (integer-order) transformation does not work. It is our proposed Theorem III (Conformality Criterion) that guarantees the necessary fraction-order transformation.

In practice, all real electrical elements may not be ideal and represent the intermediate cases between the ideal ones. As an example, we interpreted the physical origins of the asymmetric switching currents in the STT memristor. In the neural network and STT MRAM (Magnetic Random Access Memory) applications, besides the reduction of critical current, the reduction of switching asymmetry is another important issue for the proper operations.[13] The fractional memristors can also seamlessly fill the gaps between the ideal elements in the Complete Triangular Periodic Table of Elementary Circuit Elements. The position of fractional memristor in the positive or negative triangle can be found in both Figs. 7 and 15.

IV. MEM-INDUCTOR AND MEM-CAPACITOR

Memristor's variants, namely, mem-inductor or mem-capacitor, can help design ANA[18] that self-adjusts its inherent parameters (for instance, the resonant frequency) naturally following the stimuli frequency. Such an architecture is required for brain-like computers because some parameters of the stimuli (for instance, the stimuli frequency) cannot be known in advance. In principle, such adaptivity can be provided by a circuit element with memory because it is history-dependent in its behavior.

Note that memristor cannot be used directly in this case, as an RLC circuit's time constant ($\sqrt{LC}$), determining the resonant frequency, does not have any resistance term. Mem-inductor (L) or mem-capacitor (C) can ideally be used here and Fig. 13 displays the complete differential conformal transformation for mem-inductor and its delayed switching effect.[42,43] Note that mem-inductor's constitutive space is the $\int\phi$-q plane. Also note that mem-inductor and mem-capacitor are represented by the other two apexes (in addition to the memristor one) of the triangle (inset of Fig. 13).

As a hardware implementation of biological systems, ANA can be used to reproduce adaptively the observed biological phenomena in amoebae. [See Fig. 14(b) for details: the amoeba slows down when the ambient temperature drops at time points S_1, S_2, and S_3 and can, even if the temperature does not drop any longer, still predict the time of the next temperature drop by slowing down again at the times C_1, C_2, and C_3 when the drop would have occurred.][44,45] A simple RLC neuromorphic circuit using a mem-inductor, $L(q)$, was designed (Fig. 14). An input voltage, V_{in}, represents the temperature and humidity that control the motion of the amoeba, whereas an output voltage across the capacitor, V_{out}, is an analogue to amoeba's locomotive speed.

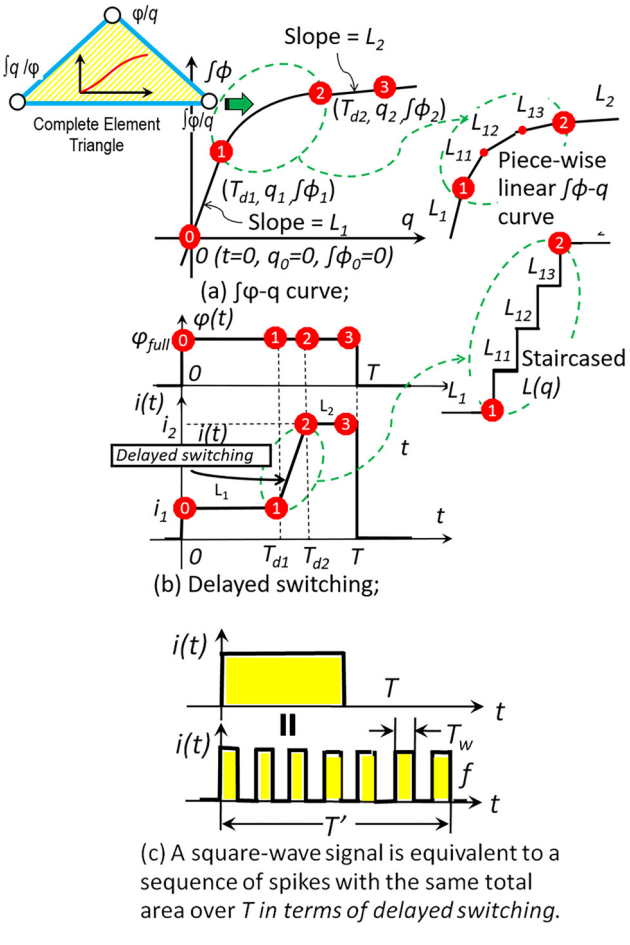

FIG. 13. The complete differential conformal transformation in the $\int\phi$-q space for mem-inductor. Mem-inductor's delayed switching effect can be seen: the switching from one state (L_1) to another (L_2) due to an input flux pulse takes place with a time delay. The effect also applies to a train of spikes ("action potentials" in neurons, i.e., short-lasting events in which the electrical membrane potential of a cell rapidly rises and falls). If the transition period (Time point 1-2) of the $\int\phi$-q curve consists of a number of linear segments, the same number of stairs in the current $i(t)$ can be generated. Reproduced with permission from Wang *et al.*, Neural Netw. **45**, 111–116 (2013). Copyright 2013 Elsevier.

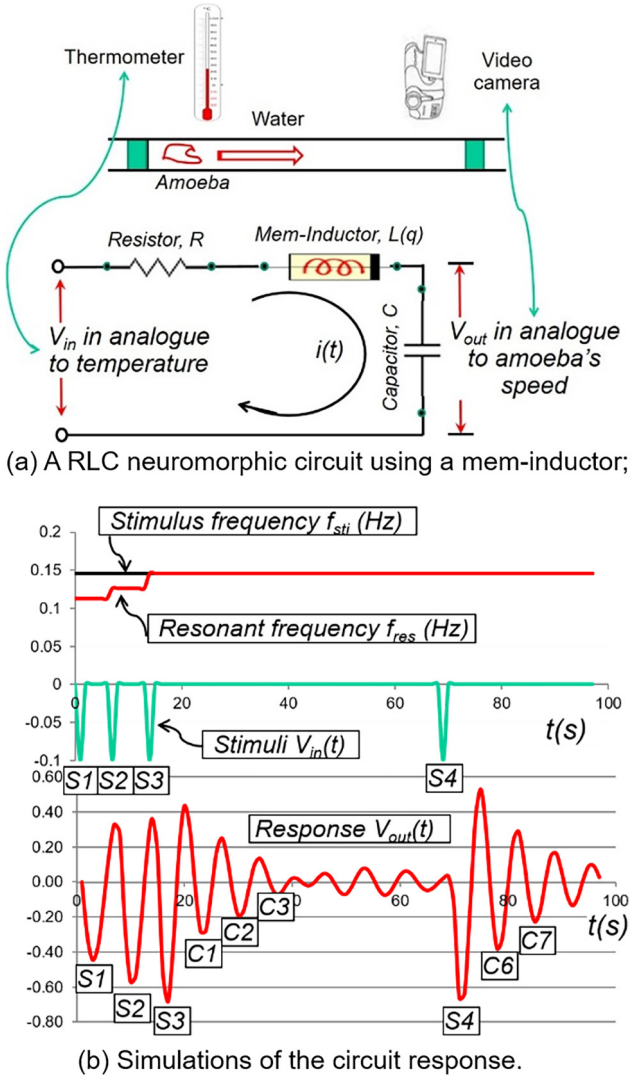

FIG. 14. A mem-inductor, $L(q)$, is used in an *RLC* neuromorphic circuit to cover a stimuli frequency with a deviation. An amoeba is put in a long tube full of fresh water at a controllable temperature measured by a thermometer. A video camera is used to measure the amoeba's migration speed. Reproduced with permission from Wang *et al.*, Neural Netw. **45**, 111–116 (2013). Copyright 2013 Elsevier.

V. NEGATIVE MEMRISTOR

A. Concept

We proposed supersymmetry in circuit theory similar to supersymmetry in particle physics (every fundamental particle has its supersymmetric particle, which is heavier than its corresponding ordinary one because supersymmetry is a broken symmetry in nature). The essence is that each elementary circuit element has a supersymmetric element which is "heavier" (due to an internal power source) than its corresponding passive one. That is to say, positive elements and negative elements are categorized into two different triangles, as shown in Fig. 15. The motivation to introduce a negative memristor is to not only complete our previously proposed triangular circuit element theory in a symmetric way but also support some real-world applications in neuromorphic computation. Concretely, negative memristor can be classified into two types.

Charge-controlled negative memristor [CCNM, Fig. 16(a)]: In this type, the flux is a single valued, continuous function of the charge, but the charge is a multivalued function of the flux. In the most common type, there is only one negative memristance region. As the charge is increased, the flux increases (positive memristance) until it reaches a maximum, then decreases in the region of negative memristance to a minimum.

Flux-controlled negative memristor [FCNM, Fig. 16(b)]: In this type, the charge is a single valued function of the flux, but the flux is a multivalued function of the charge. In the most common type, with one negative memristance region.

The following activity criterion shows what class of memristors might be synthesized in an "artifact" form with internal power supplies. For convenience, it is assumed that the ϕ-q curve passes through the origin and the left- and right-hand derivatives exist at each point.

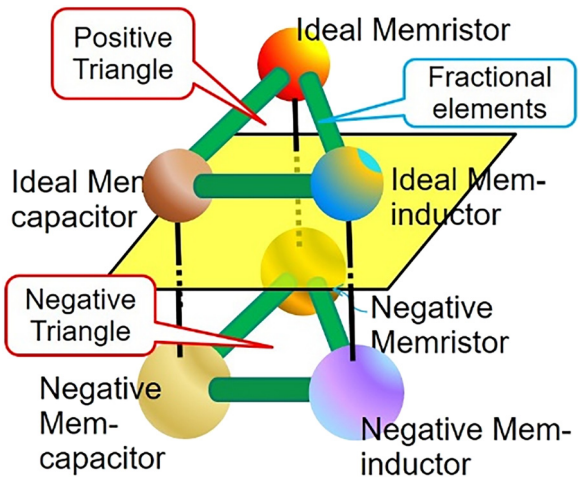

FIG. 15. The negative triangular periodic table of circuit elements and negative memristor ($\alpha = -1$). As well as other negative elements, it can symmetrically extend their (positive) counterparties to the negative space. A positive triangle includes all the positive elements, whereas a negative triangle includes all the negative ones.

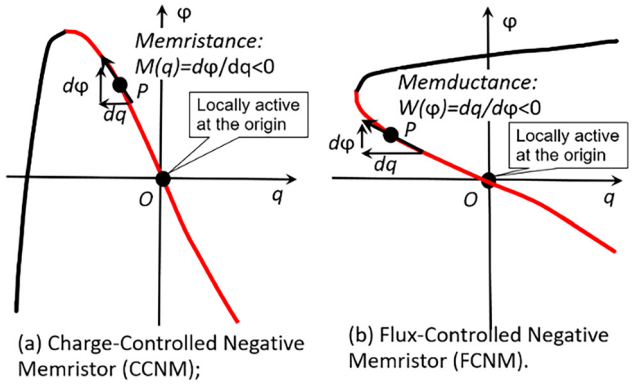

FIG. 16. ϕ-q curve of a negative or "active" memristor. Taking (a) as an example, it has negative differential memristance, $M(q) = d\phi/dq$, at the origin, i.e., is locally active (at the origin). Unlike in the conventional (positive) memristor, the downward sloping region (in red) of the ϕ-q curve passes through the origin, so it enters the 2nd and 4th quadrants of the plane, meaning the device sources power. A large enough charge or flux moves the memristor into its black region in which the differential memristance becomes positive and the memristor consumes power.

Theorem IV: Activity Criterion

A memristor characterized by a continuous charge-controlled ϕ-q curve is artifact and active if its differential memristance $M(q)$ is negative at the origin, $M(q = 0) < 0$, i.e., locally active at the origin.

Proof: The instantaneous power dissipated by a memristor is given by

$$P(t) = i(t)v(t) = M[q(t)][i(t)]^2. \tag{14}$$

Suppose that there exists a point q_0 (corresponding to t_0) such that $M(q_0) < 0$, then $P(t_0) < 0$ and the memristor is locally active[13] at that point. Because the left- and right-hand derivatives at each point on the ϕ-q curve exist, such differentiability (a continuous function need not be differentiable) implies that there exists an $\epsilon > 0$ such that $M(q_0 + \Delta q) < 0$, $|\Delta q| < \varepsilon$. If the memristor is driven by a current $i(t)$ which is zero for $t \le T$ and such that $q(t) = q_0 + \Delta q(t)$ for $t \ge t_0 \ge T$ where $|\Delta q(t)| < \varepsilon$; then $\int_{-\infty}^{t} P(\tau)d\tau < 0$ for sufficiently large t, and hence the memristor is active.[1] For convenience, the negatively sloping branch is always assumed to cross the origin so the ϕ-q curve enters the 2nd and the 4th quadrants.

This criterion shows that a negative memristor is active and artifact with a ϕ-q curve synthesized in practice by active networks. As its converse, only memristors characterized by a monotonically increasing ϕ-q curve can exist in a passive circuit element form without internal power supplies.

As shown in Fig. 17(a), a locally active memristor exhibits a negative slope at the origin of the ϕ-q curve. It follows

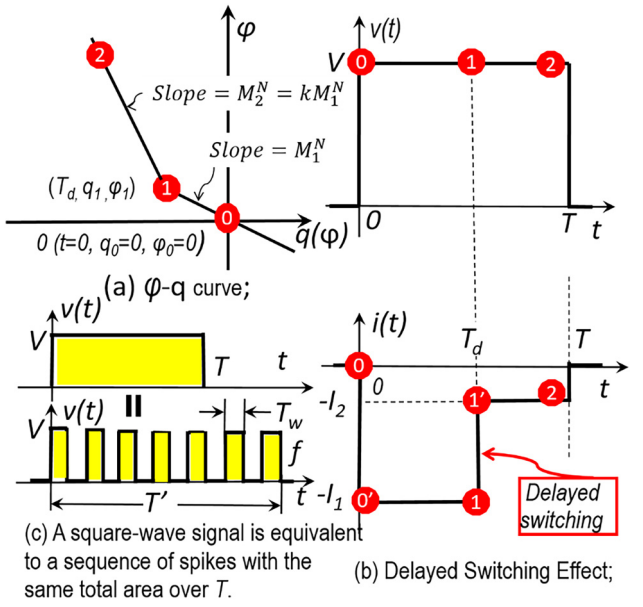

FIG. 17. A special case ($\alpha = -1$) of the complete differential conformal transformation for a (flux-controlled) negative memristor. It is defined in terms of a non-linear functional relationship between magnetic flux linkage, $\varphi(t)$, and the amount of electric charge, $q(t)$, in the 2nd and 4th quadrants of the φ-q space. In this firgure, we assume that the negative memristor is characterized by the "monotone-decreasing" and "piece-wise-linear" nonlinearity. The superscript N in the symbol for the memristance M stands for "negative." A negative memristor naturally exhibits the delayed switching. The effect also applies to a train of spikes [in (c)], well used in neuro-morphic computation.

therefore that an ideal memristor cannot exhibit a negative memristance unless it is locally active at the origin, which is possible only if the memristor has an internal source of power, such as light, chemical or nuclear reactions, or batteries. An example of this kind of active memristors is active ReRAM (which is called nanobatteries).[22]

B. Negative memristor's features

There is a vast array of literature on memristors in neural networks and/or memristive synapses after the Pershin/Ventra seminal work.[46] Our scheme of using the above negative memristor as synapses has an advantage over previous ones: it can cancel the internal membrane resistance of the neuron in some neuromorphic computation applications.

The negative memristor exhibits the delayed switching effect, as shown in Fig. 17(b). The physical interpretation of this phenomenon is that the physical attributes (such as flux and charge) of an electron element are inertial with the tendency to settle to some equilibrium state and remain unchanged.[42,43] The response cannot take place as rapidly as the variation in the excitation waveform and it always takes a finite but small time interval.

In a memristive neural network, a square-wave signal is equivalent to a sequence of spikes with the same net area in order to switch a memristor synapse [Fig. 17(c)]. The memristance M(ϕ) of a flux-controlled memristor depends on the complete past history of the voltage. Therefore,

$$\varphi(t = T_d) = \int_0^{T_d} v(\tau)d\tau = VT_d, \tag{15}$$

$$T_d = \frac{\varphi_1}{V}. \tag{16}$$

Equation (16) clearly demonstrates that the delay T_d for switching decreases with an increased spike amplitude V or a decreased ϕ_1. If the input voltage is removed before the switching takes place, the negative memristor remains unchanged. Therefore, in order to switch a negative memristor, we should take $T > T_d$. Actually, the complementary features of those positive/negative element pairs could be studied in a symmetric way.

C. Negative memristor in neuromorphic computation

Any realistic implementation of a synapse should ideally be at least four orders of magnitude smaller than that required to build a neuron (that may be connected to other neurons through about 20 000 synapses in the human brain). A $LaAlO_3/SrTiO_3$ junction presents a uni-polar pinched hysteresis loop and also shows a potential that a memristor synapse could be scaled down to half a nanometer.[47]

Similar to the recreation of Pavlov's experiment with memristor,[46] a negative memristor is used as the synapse [Fig. 18(b)] to eliminate the internal membrane resistance of the neuron in order to have an "ideal" signal source. The idea was inspired by the usage of a negative resistor in an ideal voltage source [Fig. 18(a)]. The internal longitudinal resistance of a 1 cm length of axon with a $1\,cm^2$ cross-sectional area ranges from 30 to 250 Ω.[48,49]

At the very beginning, the negative memristor M^N is programmed at $|M_1^N(\varphi)| \gg r$ to cut off the S2 link, i.e., the "Bell" stimulus alone will result in $V_O \approx 0$. In contrast, the "Sausage" stimulus can easily pass through S1 via a small r and activate the "Salivation" neuron, i.e., $V_O \approx V_S$. The training is conducted by applying both "Sausage" and "Bell" simultaneously. Consequently, a "Full Voltage" drop will be applied across the (negative memristor) synapse S2, gradually switching it from $M_1^N(\varphi)$ to $M_2^N(\varphi) = -R_M$ and establishing the conditioning during the training. After the training, the "Bell" stimulus alone can easily pass through S2 (since it is of no resistance) and elicit "Salivation," i.e., $V_O \approx V_B$. The "Sound" neuron behaves like an ideal voltage source whose voltage output does not change with the possibly changing R_{load} because its internal (membrane) resistance has been completely cancelled by the introduction of the negative memristor.

D. Circuit experiments

An electronic negative memristor synapse is implemented by the microcontroller (dsPIC30F2011) that reads the digital code from ADC and controls a switch K to connect a negative resistor out of a series to increment/decrement the

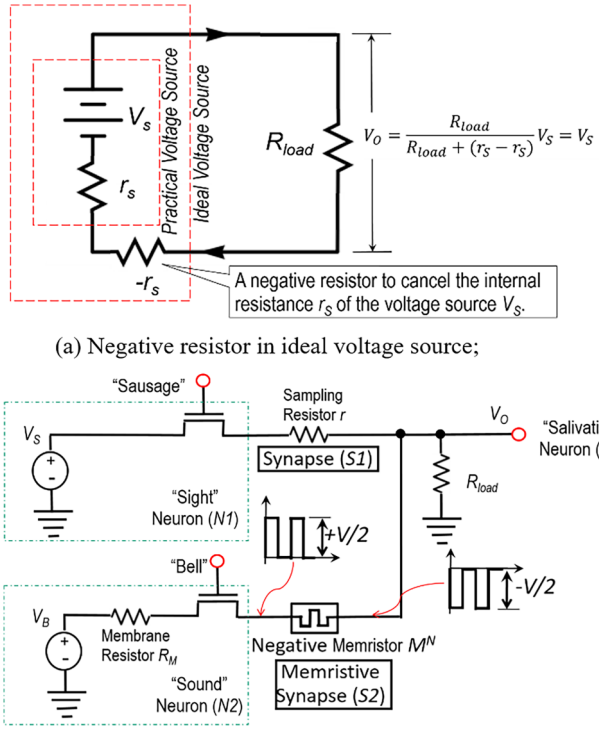

FIG. 18. A neural network using a negative memristor (M^N) to cancel the internal membrane resistance (R_M) of the neuron in (b), in a similar way to cancel the internal resistance of a voltage source by a negative resistor in (a). When a neuron fires, it starts emitting a forward spike, +V/2, and a backward spike, –V/2. The strengths of the memristive synapse can be modified (delayed switching) when these two spikes are overlapped. The synapse S_1 is realized by a simple linear resistor because the link between the "Sight" neuron and the "Salivation" neuron exists by birth.

negative memristance continuously. As shown in Fig. 19, the electronic negative memristor exhibits clearly a negative memristance and the Delayed Switching effect.

E. Negative memristor summary

We define the negative memristors based on the Activity Criterion (Theorem IV). It exhibits an ability for an active element to obtain the negative of any resistance. Locally passive memristors supplement transistors in memory functions and logic circuits with effective structures but do not satisfy all the needed requirements.[50] The sodium memristor in the Hodgkin–Huxley model is a second-order one (see Sec. I) that is passive and locally active (its locally active domain may be accessed by means of suitable battery-based biasing).[33] As the last attempt of our new memristor physics, the negative memristor not only mimics the synapses in terms of being plastic but also cancels the internal membrane resistance of the neuron in some neuromorphic computation applications.

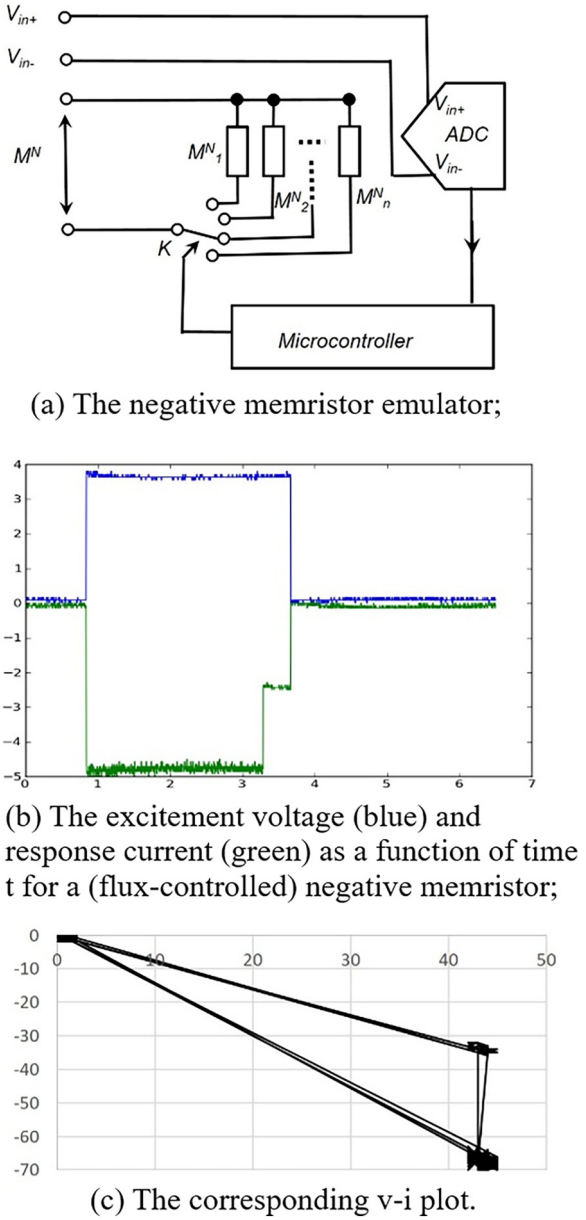

FIG. 19. An electronic negative memristor in (a) exhibits experimentally the negative memristance and the Delayed Switching effect in (b). The corresponding *v-i* plot in (c) shows a pinched hysteresis loop as the fingerprint of memristive devices. A 16-25 Hz square-wave input signal is used, the low resistance is 625 Ω, and the high resistance is 10 kΩ.

VI. CONCLUSIONS AND FUTURE WORK

This article focuses on new memristor physics that enables brain-like functionality for neuromorphic computation and memory (attributing to memristor's 2-in-1 feature) with significantly reduced power usage (attributing to memristor's

passivity), while also enabling dense highly connected networks (attributing to memristor's simple structure and small size).

The invention of memristor and its variants (ideal memristor, fractional memristor, mem-inductor, mem-capacitor, negative memristor, etc.) opens a new way to unveil the physics of the operations of the human brain and possibly of many other adaptive and spontaneous behaviors/mechanisms in living organisms. As a useful 3-in-1 physical model, our developed flux-charge-interaction-based ideal Φ memristor (Fig. 1), the complete differential conformal transformation (Figs. 6 and 11), and the complete triangular periodic table of elementary circuit elements (Fig. 7) cover all cases in this article: $\alpha = 1$ corresponds to a (positive) ideal Φ memristor (Sec. II); $-1 < \alpha < 1$ corresponds to a (positive/negative) fractional memristor (Sec. III); the above classification also applies to the mem-inductor/mem-capacitor families in their own constitutive spaces (Sec. IV); $\alpha = -1$ corresponds to a negative (ideal) memristor (Sec. V). The first three elements are passive, whereas the last one is active.

We hope to elaborate this 3-in-1 physics in a more coherent way: The deduced Eq. (6) (and its approximations) for the Φ memristor (the 1st component of the 3-in-1 physics) is used as the basic flux-charge relationship in the complete conformal differential transformation (the 2nd component); the generic formula for the fractional memristor (and its extensions) deduced in the complete transformation (the 2nd component) is used to label those fractional elements in the complete triangular table of basic circuit elements (the 3rd component).

Our memristor-based neuromorphic computation is technically positioned between the brain and the traditional computer, as shown in Fig. 20. We are pushing it toward the brain direction. (Brains are thought to be made of memristors.[33]) In Fig. 20, the traditional Turing machine is represented as two boxes: CPU and memory. Historically, such a separation of computation and memory simplifies the machine design and exceeds the natural human brain in terms of computational performance. However, there are two sides to everything. There are two negative side-effects: the communication overhead between the two boxes (CPU and memory) and the energy consumption that may be several orders of magnitude larger. By nature, memristor (as well as its variants) is a 2-in-1 element combining both memory and computation functions. The Adaptive Neuromorphic Architecture (ANA) in Sec. IV is a remarkable example, in which a mem-inductor can not only memorize the past history of the stimuli but also compute the time constant ($\sqrt{LC}$). That is why we see a small energy consumption in the brain (it consumes only about the same amount of electric power as a night light) in contrast to that of the traditional architecture.

As a piece of work-in-progress in our labs, the Spin Hall Memristive (SHM) effect is predicted based on a similar structure in Fig. 1: a piece of ferromagnetic conductor with two terminals. The structure facilitating the predicted Spin Hall Memristive (SHM) effect is a ferromagnetic conductor with two terminals (Fig. 21). The electricity-magnetism interaction is needed for an ideal memristor, as discussed in Sec. I. A ferromagnet is expected to provide a good source of nonlinearity for the memristive effect from its rich hysteresis. The spin Hall effect (SHE[51–53]) is expected to be a good source of spin current. The induced spin current is expected to switch the ferromagnet efficiently via Spin-Torque Transfer (STT).[17,18]

At this stage, its classic implementation (via Oersted's field) was experimentally studied and the most important memristive mechanism was verified, as reported in Sec. II. We think this is a new electro-magnetic effect with the clear physical origin and great application potential in electron devices. By our theory, the SHM effect should, at the nanoscale

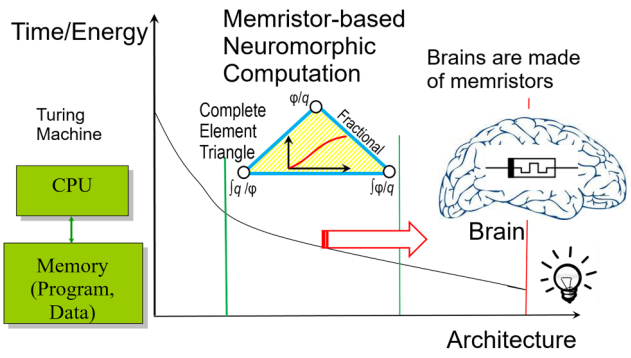

FIG. 20. Our memristor-based neuromorphic computation is technically positioned between the brain and the traditional computer. Brains are thought to be made of memristors. By nature, memristor is a 2-in-1 element combining both memory and computation functions.

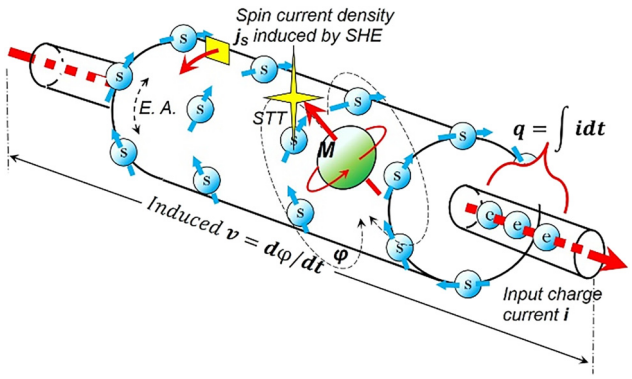

FIG. 21. The Spin Hall Memristive (SHM) Effect. SHE (Spin Hall Effect) converts an input (charge) current i flowing through the conductor to a spin current winding around the cylindrical surface, like the lines of the magnetic field $\boldsymbol{H}$ produced by i. The boundary spin polarization changes sign when the direction of the input charge current is reversed. The induced spin current can exert directly torque via STT upon the magnetization $\boldsymbol{M}$ of the ferromagnet and switch it. Consequently, the switched flux φ induces a voltage v across the two terminals, resulting in a changed (equivalent) memristance whose value is a function of the history of i.

for its quantum implementation, be four orders of magnitude larger than its classic implementation. The (equivalent) magnetic field generated by the spin current j via STT is expected to play the same role as Oersted's field to generate the memristive effect although the latter may be much smaller than the former, especially when the Giant Spin Hall effect[54,55] is used.

Searching for materials that suit all the 3 mechanisms (namely, the electricity-magnetism interaction, SHE, and STT) in the SHM effect may be challenging. As to SHE itself, it has taken 33 years to observe the effect experimentally in the gallium arsenide/indium gallium arsenide samples[53] since the SHE effect was predicted in 1971.[51]

ACKNOWLEDGMENTS

This research was partially conducted in an EC grant "Re-discover a periodic table of elementary circuit elements," No. PIIF-GA-2012-332059, Marie Curie Fellow: Professor Leon Chua, Scientist-in-Charge: Professor Frank Wang.

REFERENCES

[1]L. Chua, "Memristor—The missing circuit element," IEEE Trans. Circ. Theory CT **18**(5), 507–519 (1971).
[2]L. Chua, "Resistance switching memories are memristors," Appl. Phys. A **102**, 765 (2011).
[3]L. Chua, "If it's pinched it's a memristor," Semicond. Sci. Technol. **29**, 104001 (2014).
[4]L. Chua, "Nonlinear circuit foundations for nanodevices. Part I: The four-element torus," Proc. IEEE **91**(11), 1830–1859 (2003).
[5]F. Z. Wang, "A triangular periodic table of elementary circuit elements," IEEE Trans. Circ. Syst. **60**(3), 616 (2013).
[6]D. Strukov, G. Snider, D. Stewart, and S. Williams, "The missing memristor found," Nature **453**, 80–83 (2008).
[7]E. Gale, "The memory-conservation theory of memristance," in *2014 UKSim-AMSS 16th International Conference on Computer Modelling and Simulation, Cambridge, UK, 26-28 March 2014* (IEEE, 2014).
[8]S. Vongehr, "Missing the memristor," Adv. Sci. Lett. **17**, 285 (2012).
[9]S. Vongehar and X. Meng, "The missing memristor has not been found," Nat. Sci. Rep. **5**, 11657 (2015).
[10]See https://en.wikipedia.org/wiki/Flux_linkage for flux linkage; accessed 15 November 2018.
[11]L. D. Landau and E. M. Lifshitz, "Theory of the dispersion of magnetic permeability in ferromagnetic bodies," Phys. Z. Sowjetunion. **8**, 153 (1935).
[12]T. L. Gilbert, "A Lagrangian formulation of the gyromagnetic equation of the magnetic field," Phys. Rev. **100**, 1243 (1955).
[13]F. Z. Wang, L. Shi, H. Wu, N. Helian, and L. O. Chua, "Fractional memristor," Appl. Phys. Lett. **111**, 243502 (2017).
[14]K. B. Oldham and J. Spanier, *The Fractional Calculus* (Academic Press, New York, 1974).
[15]I. Podlubny, *Fractional Differential Equations* (Academic Press, San Diego, 1999).
[16]J. C. Slonczewski, "Current-driven excitation of magnetic multilayers," J. Magn. Magn. Mater. **159**, l1–2 (1996).
[17]L. Berger, "Emission of spin waves by a magnetic multilayer traversed by a current," Phys. Rev. B **54**, 9353 (1996).
[18]F. Z. Wang, L. O. Chua, X. Yang, N. Helian, R. Tetzlaff, T. Schmidt, L. Li, J. M. Carrasco, W. Chen, and D. Chu, "Adaptive Neuromorphic Architecture (ANA)," Neural Netw. **45**, 111–116 (2013).
[19]K. Mainzer and L. Chua, *Local Activity Principle* (Imperial College Press, 2013).
[20]A. Aharoni, *Introduction to the Theory of Ferromagnetism*, 2nd ed. (Clarendon Press, 1996), pp. 330–336.
[21]L. Chua, in *Keynote speech, 1st International Symposium of Brain-like Computing: Memristor Devices and Systems, Beijing*, 1 December 2017 (Peking University, 2017).
[22]I. Valov, E. Linn, S. Tappertzhofen, S. Schmelzer, J. van den Hurk, F. Lentz, and R. Waser, "Nanobatteries in redox-based resistive switches require extension of memristor theory," Nat. Commun. **4**, 1771 (2013).
[23]M. Julliere, "Tunneling between ferromagnetic films," Phys. Lett. A **54**, 225–226 (1975).
[24]T. Prodromakis, C. Toumazou, and L. Chua, "Two centuries of memristors," Nat. Mater. **11**, 478–481 (2012).
[25]V. Erokhin, G. D. Howard, and A. Adamatzky, "Organic memristor devices for logic elements with memory," Int. J. Bifurcation Chaos **22**(11), 1250283 (2012).
[26]L. V. Gambuzza, L. Fortuna, M. Frasca, and E. Gale, "Experimental evidence of chaos from memristors," Int. J. Bifurcation Chaos **25**(8), 1550101 (2015).
[27]N. Gergel-Hackett, B. Hamadani, B. Dunlap, J. Suehle, C. Richter, C. Hacker, and D. Gundlach, "A flexible solution-processed memristor," IEEE Electron Device Lett. **30**(7), 706-708 (2009).
[28]M. J. Donahue and D. G. Porter, "Analysis of switching in uniformly magnetized bodies," IEEE Trans. Magn. **38**(5), 2468–2470 (2002).
[29]E. M. Gyorgy, "Rotational model of flux reversal in square loop ferrites," J. Appl. Phys. **28**(9), 1011–1015 (1957).
[30]N. Cushman, "Characterization of magnetic switch cores," IRE Trans. Comp. Parts **8**(2), 45–50 (1961).
[31]N. Menyuk and J. Goodenough, "Magnetic materials for digital computer components I," J. Appl. Phys. **26**(1), 8 (1955).
[32]P. S. Georgiou, M. Barahona, S. N. Yaliraki, and E. M. Drakakis, "On memristor ideality and reciprocity," Microelectron. J. **45**, 1363–1371 (2014).
[33]L. Chua, V. Sbitnev, and H. Kim, "Hodgkin–Huxley axon is made of memristors," Int. J. Bifurcation Chaos **22**, 1230011 (2012).
[34]X. Wang, Y. Chen, H. Xi, H. Li, and D. Dimitrov, "Spintronic memristor through spin-torque-induced magnetization motion," IEEE Electron Device Lett. **30**(3), 294–297 (2009.
[35]H. Oersted, *Experiments on the Effect of a Current of Electricity on the Magnetic Needles* (Annals of Philosophy, London, 1820).
[36]G. S. Ohm, *Die Galvanische Kette, Mathematisch Bearbeitet* (Riemman, 1827), Vol. **250**.
[37]M. Faraday, *Experimental Researches in Electricity* (Bernard Quaritch, 1833).
[38]H. B. Huang, X. Q. Ma, T. Yue, Z. H. Xiao, S. Q. Shi, and L. Q. Chen, "Magnetization switching modes in nanopillar spin valve under the external field," Sci. China: Phys., Mech. Astron. **54**, 1227-1234 (2004).
[39]Y. Huai, D. Apalkov, Z. Diao, Y. Ding, and A. Panchula, "Structure, materials and shape optimization of magnetic tunnel junction devices: Spin-transfer switching current reduction for future magnetoresistive random access memory," Jpn. J. Appl. Phys. **45**(5A), 3835–3841 (2006).
[40]X. Li, Z. Zhang, Q. Y. Jin, and Y. Liu, "Spin-torque-induced switching in a perpendicular GMR nanopillar with a soft core inside the free layer," New J. Phys. **11**, 023027 (2009).
[41]H. Meng and J. Wang, "Asymmetric spin torque transfer in nano GMR device with perpendicular anisotropy," IEEE Trans. Magn. **43**(6), 2833–2835 (2007).
[42]F. Z. Wang, N. Helian, S. Wu, M. Lim, Y. Guo, and A. Parker, "Delayed switching in memristors and memristive systems," IEEE Electron Device Lett. **31**(7), 755–757 (2010).
[43]F. Z. Wang, N. Helian, Y. Guo, S. Wu, X. Yang, M. Lim, and M. Rashid, "Delayed switching applied to memristor neural networks," J. Appl. Phys. **111**(7), 07E317-1–07E317-3 (2011).
[44]T. Saigusa, A. Tero, T. Nakagaki, and Y. Kuramoto, Phys. Rev. Lett. **100**, 018101 (2008).
[45]Y. V. Pershin, S. La Fontaine, and M. Di Ventra, "Memristive model of amoeba learning," Phys. Rev. E **80**, 021926 (2009).
[46]Y. Pershin and M. D. Ventra, "Experimental demonstration of associative memory with memristive neural networks," Neural Netw. **23**, 881–886 (2010).
[47]T. Fix, J. MacManus-Driscoll, and M. Blamire, "Delta-doped LaAlO3/SrTiO3 interfaces," Appl. Phys. Lett. **94**, 172101 (2009).

[48]L. Hahn, see http://retina.anatomy.upenn.edu/~rob/lance/model_compartment.html for compartmental models (1995).
[49]Y. Wang, W. Fei, and H. Yu, "SPICE simulator for hybrid CMOS memristor circuit and system," in *13th International Workshop on Cellular Nanoscale Networks and Their Applications* (CNNA), *Turin*, *Italy*, 29–31 August 2012 (Politecnico di Torino, 2012), pp. 1–6, ISSN: 2165-0160.
[50]M. Itoh and L. Chua, "Memristor oscillators," Int. J. Bifurcation Chaos **18**(11), 3183–3206 (2008).
[51]M. Dyakonov and V. Perel, "Possibility of orienting electron spins with current," Sov. Phys. JETP Lett. **13**(11), 657–660 (1971).
[52]M. Dyakonov, see https://arxiv.org/pdf/1210.3200 for "Spin Hall effect" (2012), accessed 16 November 2018.
[53]K. Kato, R. Myers, A. Gossard, and D. Awschalom, "Observation of the spin hall effect in semiconductors," Sci. **306**(5703), 1910–1913 (2004).
[54]L. Liu, C. Pai, Y. Li, H. Tseng, D. Ralph, and R. Buhrman, "Spin torque switching with the giant spin Hall effect of tantalum," Science **336**(6081), 555–558 (2012).
[55]C. Pai, L. Liu, Y. Li, H. Tseng, D. Ralph, and R. Buhrman, "Spin transfer torque devices utilizing the giant spin Hall effect of tungsten," Appl. Phys. Lett. **101**(12), 2404 (2012).